Transport in Porous Media (2006) 64: 103–121
DOI 10.1007/s11242-005-1525-8

Acoustically Enhanced Ganglia Dissolution and Mobilization in a Monolayer of Glass Beads

CONSTANTINOS V. CHRYSIKOPOULOS[1,⋆] and ERIC T. VOGLER[2]
[1]*Department of Civil Engineering, University of Patras, Patras, 26500, Greece*
[2]*Department of Civil and Environmental Engineering, University of California, Irvine, CA 92697, USA*

(Received: 25 March 2005; in final form: 1 August 2005)

Abstract. A pore network consisting of a monolayer of glass beads was constructed for experimental investigation of the effects of acoustic waves on the dissolution and mobilization of perchloroethylene (PCE) ganglia. Dissolution experiments were conducted with acoustic wave frequencies ranging from 75 to 225 Hz at a constant pressure amplitude of 3.68 kPa applied to the inlet of the monolayer. Ganglia mobilization experiments were conducted with a constant acoustic wave frequency of 125 Hz and acoustic pressure amplitudes ranging from 0 to 39.07 kPa. Effluent dissolved PCE concentrations were observed to increase in the presence of acoustic waves with the greatest increase (over 300%) occurring at the lowest frequency employed (75 Hz). Acoustic waves were also observed to mobilize otherwise immobile PCE ganglia, break them apart, and further enhance dissolution.

Key words: NAPL dissolution, ganglia mobilization, monolayer of glass beads, pore network, perchloroethylene, acoustic waves, enhanced dissolution.

Notation

A_i	ith NAPL-water interfacial area (L^2)
C	aqueous phase solute concentration (M/L^3)
C_s	equilibrium aqueous solubility (M/L^3)
$\overline{C}$	average concentration (M/L^3)
$\overline{C}_a$	average effluent concentration in presence of acoustic waves (M/L^3)
$\overline{C}_b$	average effluent concentration in the absence of acoustic waves (M/L^3)
d_p	mean particle/glass-bead diameter (L)
$\mathcal{D}$	molecular diffusion coefficient (L^2/t)
F_b	buoyant force (F)
F_c	net capillary restraining force (F)
F_v	viscous force (F)
J	mass flux (M/L^2t)
J_i	mass flux at interface i (M/L^2t)
k	mass transfer coefficient (L/t)
k_e	effective mass transfer coefficient (L/t)
ℓ	boundary layer thickness (L)

⋆Author for correspondence: e-mail: gios@upatras.gr

L_g length of a ganglion (L)
N_{Ca} Capillary number (–)
N_i mass transfer rate from interface i (M/t)
p_e acoustic effluent pressure (F/L^2)
p_s acoustic source pressure (F/L^2)
P_c capillary pressure (F/L^2)
P_{Ca} advancing interface capillary pressure (F/L^2)
P_{Cr} receding interface capillary pressure (F/L^2)
P_o pressure in DNAPL phase (F/L^2)
P_w pressure in aqueous phase (F/L^2)
Q volumetric fluid flow rate (L^3/t)
r_1, r_2 principle radii of interfacial curvature (L)
r_H hydraulic radius (L)
t time (t)
U_w average interstitial pore water velocity (L/t)
V porous medium elementary volume (L^3)

Greek letters

β solid–liquid–liquid interface contact angle (°)
$\Delta\overline{C}$ percent change in average effluent concentration (%)
ΔP_c difference in advancing and receding interface capillary pressure, (F/L^2)
θ porosity (–)
μ_w dynamic viscosity of water (Ft/L^2)
σ_{ow} interfacial tension between nonaqueous and aqueous phase liquids (F/L)
ϕ acoustic wave frequency (1/t)

1. Introduction

The accidental release of non-aqueous phase liquids (NAPLs) in the subsurface impacts groundwater quality and poses a great risk to human health. The removal of DNAPLs from groundwater aquifers is a challenging task because these liquids are only slightly soluble in water (Mercer and Cohen, 1990; Khachikian and Harmon, 2000) and their dissolution is very slow and mass transfer limited (Powers *et al.*, 1991; Chrysikopoulos, 1995; Dela Bare *et al.*, 2002).

Traditionally, the remediation of residual dense nonaqueous phase liquids (DNAPLs) in saturated subsurface formations is performed by pump-and-treat methodologies. Unfortunately, groundwater velocities and hydraulic gradients associated with pumping are not great enough to sufficiently mobilize ganglia (Wilson *et al.*, 1990). Other technologies for DNAPL remediation employ the combined use of surfactants and/or cosolvents with the pump-and-treat methodology, air sparging, bio-remediation, and natural attenuation (Abriola *et al.*, 1993; Brandes and Farley, 1993; Pennell *et al.*, 1994; Seagren *et al.*, 1994; Chaudhry, 1994; Imhoff *et al.*, 1995; Fortin *et al.*, 1997; Rao *et al.*, 1997; Boving *et al.*, 1999; Grubb and

Sitar, 1999; Tatalovich *et al.*, 2000; Saba *et al.*, 2001; Hofstee *et al.*, 2003). However, these methods may introduce additional non-potable chemicals to groundwater, they are only effective at shallow depths, or they are time consuming to be considered as viable remediation technologies when groundwater demand is urgent.

For direct observation of DNAPL ganglia dissolution and mobilization in conjunction with the various alternative remediation methods, experimental studies at the pore scale are often performed. However, the majority of recent investigations on DNAPL ganglia at the pore scale within network models have been primarily focused on various entrapment and mobilization processes (Lenormand *et al.*, 1983; Dias and Payatakes, 1986; Hinkley *et al.*, 1987; Lenormand, 1990; Fenwick and Blunt, 1998) as well as dissolution mechanisms (Kennedy and Lennox, 1997; Jia *et al.*, 1999; Dillard and Blunt, 2000; Knutson *et al.*, 2001; Sahloul *et al.*, 2002; Tsakiroglou *et al.*, 2003; Zhao and Ioannidis, 2003) as a function of capillary pressure, pore structure and interfacial tension.

A unique method for enhanced DNAPL remediation incorporates the use of acoustic waves. Experimental studies have shown that acoustic waves enhance dissolved mass transport in saturated porous media (Vogler and Chrysikopoulos, 2002), and also increase dissolution/mass-transfer from single and multicomponent DNAPL ganglia in saturated porous media (Chrysikopoulos and Vogler, 2004; Vogler and Chrysikopoulos, 2004). Furthermore, several other investigations indicated that vibration of porous media can mobilize DNAPL ganglia (Reddi and Challa, 1994; Reddi and Wu, 1996; Reddi *et al.*, 1998; Roberts *et al.*, 2001). Consequently, it is reasonable to assume that acoustic waves can also affect the mass transfer rate and mobilization of DNAPL ganglia in porous media. The purpose of this work is to investigate how acoustic waves can alter the dissolution and mobilization of perchloroethylene (PCE) ganglia in a two-dimensional monolayer network of 3 mm diameter soda lime glass beads. The major advantage of monolayer networks over frequently employed packed columns is that monolayers allow for direct observation of the movement and geometry changes of the various ganglia at the pore scale.

2. Theory

2.1. GANGLIA DISSOLUTION

NAPL dissolution in water saturated porous media is governed mainly by mass transfer across NAPL–water interfaces (Chrysikopoulos *et al.*, 2002, 2003). Consequently, for a NAPL ganglion trapped by capillary forces at pore constrictions, as illustrated in Figure 1, pore throats adjacent to NAPL–water interfaces can act as conduits for dissolved aqueous phase

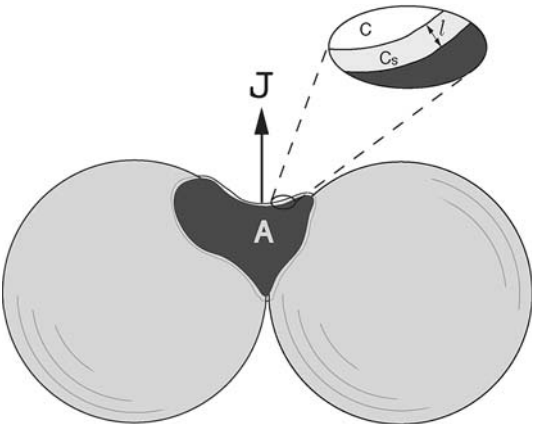

Figure 1. Schematic of a ganglion trapped between two glass beads showing the NAPL–water interfacial area, A, the perpendicular to the interface mas flux, J, the stagnant concentration boundary layer thickness, ℓ, the aqueous solubility concentration at the interface C_s, and the aqueous concentration, C.

NAPL mass transport between pores. Assuming that a stagnant concentration boundary layer forms over the NAPL–water interface, the mass flux per unit interfacial area is given by (Kim and Chrysikopoulos, 1999)

$$J = -\mathcal{D}\frac{(C - C_s)}{\ell} = k(C_s - C), \tag{1}$$

where J is the mass flux perpendicular to the NAPL–water interfacial area, $\mathcal{D}$ the molecular diffusion coefficient, C_s the aqueous concentration at the interface and for a pure phase organic liquid is equal to the liquid's aqueous saturation or solubility concentration (Chrysikopoulos *et al.*, 1994; Seagren *et al.*, 1994), C the aqueous phase concentration of the dissolved NAPL outside the boundary layer in the pore, ℓ the boundary layer thickness, and k is the local mass transfer coefficient. The first formulation in (1) represents the diffusive mass flux into the boundary layer at the NAPL–water interface given by Fick's law (Cussler, 1984, p. 23), whereas the latter formulation represents the convective mass transfer flux. Convective mass transfer occurs when $C_s \neq C$, and is analogous to Newton's law of cooling (Bird *et al.*, 1960, p. 267). The preceding equation implies that dissolution at a NAPL–water interface is limited only by the mass transfer of the dissolved solute, and that the local mass transfer coefficient can be expressed as

$$k = \frac{\mathcal{D}}{\ell}. \tag{2}$$

For a representative elementary volume V of a porous medium containing several ganglia and consequently various NAPL–water interfaces, the macroscopic scale mass transfer can be expressed as (Held and Celia, 2001)

$$\frac{1}{V}\sum_{i} Ni = k_{\mathrm{e}}(C_{\mathrm{s}} - \overline{C}), \tag{3}$$

where

$$N_i = J_i A_i, \tag{4}$$

is the mass transfer rate from the ith NAPL–water interface; A_i the ith NAPL–water interfacial area; k_{e} is the effective mass transfer rate coefficient, and $\overline{C}$ is the average aqueous phase concentration of the dissolved NAPL within the representative elementary volume.

2.2. GANGLIA MOBILIZATION

The migration of ganglia in porous media is a relatively complex process that has received considerable attention by petroleum, chemical, and environmental engineers (Ng *et al.*, 1978; Payatakes, 1982; de la Cruz and Spanos, 1983; Hinkley *et al.*, 1987; Lenormand and Zarcone, 1988; Morrow *et al.*, 1988; Blunt and King 1992; Mayer and Miller, 1993; Avraam and Payatakes, 1995; Pennell *et al.*, 1996; Bradford *et al.*, 2003). For a single immobile ganglion, there is a pressure discontinuity at the curved water–NAPL interface. The difference between the local pressure in the NAPL, P_{o}, and the pressure in the water, P_{w}, on a single meniscus is the capillary pressure,

$$P_{\mathrm{c}} = P_{\mathrm{o}} - P_{\mathrm{w}}. \tag{5}$$

The magnitude of P_{c} depends on the meniscus curvature and may be described by the Young-Laplace equation (Bear, 1972, p. 445):

$$P_{\mathrm{c}} = \sigma_{\mathrm{ow}}\left(\frac{1}{r_1} + \frac{1}{r_2}\right), \tag{6}$$

where σ_{ow} is the interfacial tension between the nonaqueous and aqueous phase liquids, and r_1 and r_2 are the principle radii of curvature of the interface. For complicated solid structures, such as those encountered in subsurface formations, the capillary pressure may be represented as (Bear, 1972, p. 446):

$$P_{\mathrm{c}} = \frac{\sigma_{\mathrm{ow}}\cos\beta}{r_{\mathrm{H}}}, \tag{7}$$

where β is the contact angle of the solid–liquid–liquid interface, and r_{H} is the hydraulic radius of the capillary which is equivalent to the ratio of void volume to surface area of the porous medium. For the case of a porous

medium composed of uniform spherical particles, the hydraulic radius may be defined as (Dullien, 1979, p. 255; Dawson, 1992, p. 11):

$$r_{\mathrm{H}} = \frac{\theta d_{\mathrm{p}}}{6(1-\theta)}, \tag{8}$$

where d_{p} is the mean particle diameter; and θ is the porosity of the porous medium.

The solitary immobile NAPL ganglion with length L_{g} shown in Figure 2a can advance one pore space, as shown in Figure 2b, only if the viscous force, F_{v}, of the interstitial water moving from left to right past the ganglion plus the buoyant force, F_{b}, exceed the restraining net capillary force, F_{c}:

$$F_{\mathrm{v}} + F_{\mathrm{b}} \geqslant F_{\mathrm{c}}. \tag{9}$$

Moreover, the difference in capillary pressure between the advancing and receding interfaces

$$\Delta P_{\mathrm{c}} = P_{\mathrm{c_a}} - P_{\mathrm{c_r}}, \tag{10}$$

where the subscripts a and r denote the advancing and receding interfaces, respectively, must be overcome (Ng *et al.*, 1978).

Experimental determination of the various parameters associated with Equations (9) and (10) is not a trivial task. For the case of horizontal mobilization examined in this study, gravity is neglected, and consequently the principal ganglia mobilization criteria are traditionally presented by the dimensionless capillary number N_{Ca}. The capillary number is the ratio of viscous to capillary forces and is defined as (Dawson and Roberts, 1997):

$$N_{\mathrm{Ca}} = \frac{U_{\mathrm{w}}\mu_{\mathrm{w}}}{\sigma_{\mathrm{ow}} \cos\beta}, \tag{11}$$

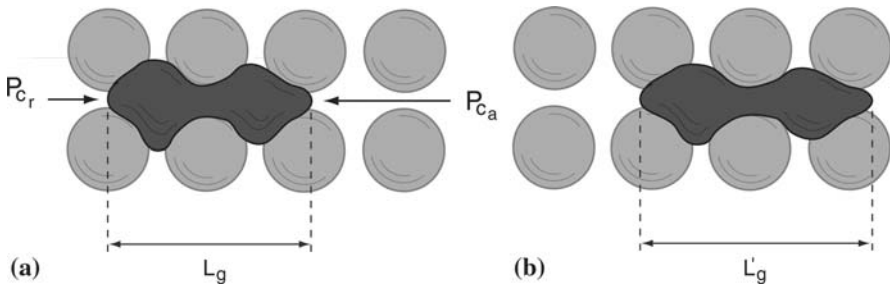

Figure 2. Schematic illustration of a two-pore volume ganglion migrating from its initial location (a) to one pore space downstream (b). The length of the ganglion before and after its mobilization is L_g and L'_g, respectively ($L'_g > L_g$). The advancing and receding capillary pressures are indicated by $P_{\mathrm{c_a}}$ and $P_{\mathrm{c_r}}$, respectively.

where U_w is the average interstitial pore water velocity; and μ_w is the dynamic viscosity of water. It should be noted that for strongly water-wet systems it is often assumed that $\cos\beta = 1$ (Blunt *et al.*, 2002).

It has been shown that ganglia mobilization is highly dependent on N_{Ca}. The average ganglion velocity increases monotonically with increasing N_{Ca}. Once in motion, the ganglia tend to align themselves with the overall flow direction and when confronted with a bifurcation they continue a regular zig-zag motion (Hinkley *et al.*, 1987). With increasing N_{Ca}, ganglia begin to break up into many individual singlets. This formation of NAPL singlets is referred to as dynamic breakup (Payatakes, 1982). The conditions for ganglia mobilization have been thoroughly summarized by Dawson (1992).

3. Experimental Design and Procedures

3.1. MONOLAYER OF GLASS BEADS

To determine the effect of acoustic waves on DNAPL ganglia dissolution and mobilization, a two-dimensional monolayer network of 3 mm diameter soda lime glass beads (Fisher Scientific, Pennsylvania) was designed and constructed. Although etched glass micromodels have been effectively used to study two-phase immiscible flow (e.g., Avraam *et al.*, 1994), a monolayer of glass beads is employed in this work to closer approximate DNAPL migration in real porous media. Experience gained from previous studies with etched glass micromodels (Buckley, 1991; Li and Yortsos, 1995; Keller *et al.*, 1997; Jia *et al.*, 1999; Chomsurin and Werth, 2003; Tsakiroglou *et al.*, 2003; Zhao and Ioannidis, 2003) was utilized in the present study in order to design and build the best possible monolayer of glass beads.

The monolayer network of glass beads was contained within a specially designed plexiglass device. An aluminum structure was used to hold the plexiglass device and to provide support for the acoustic transducer. A recess in the plexiglass device allowed space for the glass beads and two glass plates. The 6.35 mm (1/4 in.) borosilicate glass plates were placed on top and bottom of the glass beads and they were surrounded by stainless steel retainers. The retainers kept the bottom glass plate and beads in place within the recess of the plexiglass device, and directed the fluid flow and acoustic pressure through the monolayer of glass beads. Holes were drilled through the top glass at 45°, which were used as NAPL ganglia injection ports. The injection ports were sealed (water tight) with clear silicone sealant. The top glass plate was held in place with a plexiglass retainer with a cut out center to allow for clear viewing of the glass beads. A 1.59 mm (1/16 in.) thick santoprene sheet with a cut out center was placed between the plexiglass retainer and the base of the monolayer device. A picture of the monolayer device is shown in Figure 3.

Acoustic pressure was delivered to the monolayer device with a diaphragm attached to the acoustic source transducer (TST37; Clark Synthesis, Colorado). Flow of degassed Millipore water was maintained through the monolayer with a microprocessor pump drive (Cole Palmer Instrument Co., Illinois). The frequency of acoustic pressure oscillation was controlled by a frequency generator (LG Precision, California). Acoustic pressure levels were controlled by an amplifier (Lab Gruppen, Sweden) and measured using two PCB106b pressure sensors (PCB Piezotronics Inc., New York). The pressure sensors were installed within the monolayer device on the influent and effluent sides. Pressure sensor measurements were made using a signal conditioner (PCB Piezotronics Inc., New York) in addition to a digital multimeter (Metex, Korea) and an oscilloscope (EZ Digital Co., Ltd, Korea). A complete schematic illustration of the experimental apparatus is shown in Figure 4.

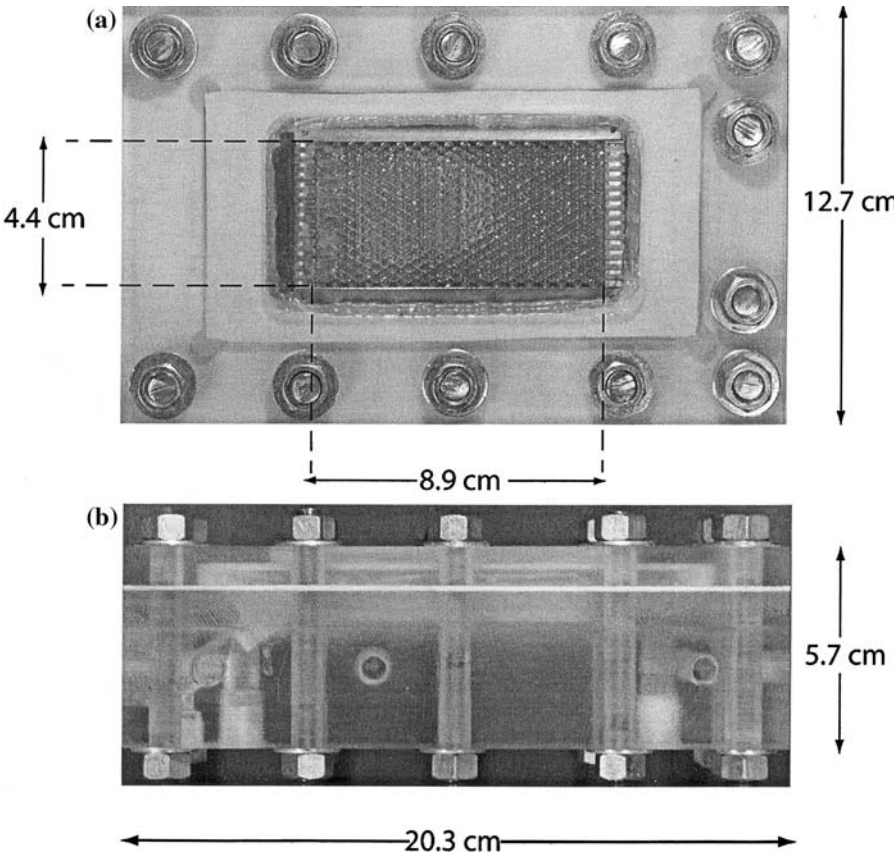

Figure 3. Pictures of the (a) top view and (b) side view of the monolayer device.

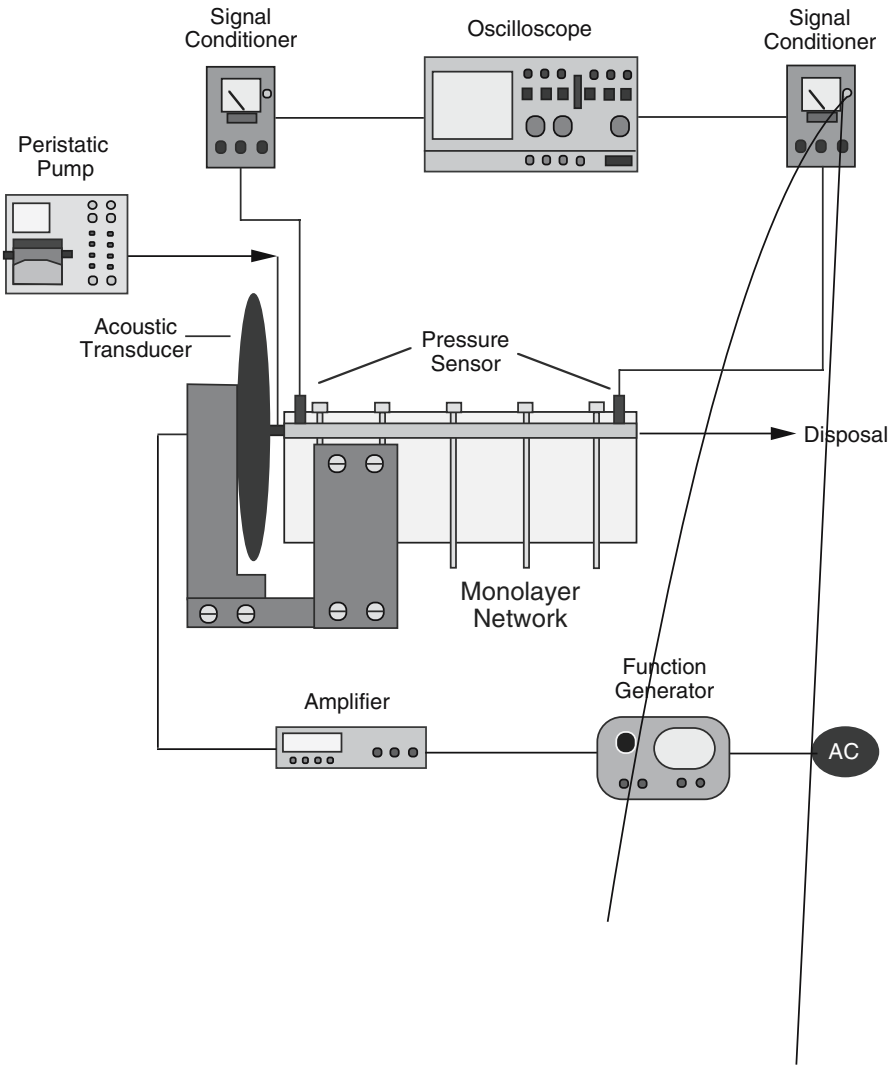

Figure 4. Schematic illustration of the experimental setup.

3.2. EXPERIMENTAL PROCEDURES FOR GANGLIA DISSOLUTION

DNAPL ganglia dissolution experiments were initiated by injecting 0.05 mL of tetrachloroethylene (PCE) (Fisher Scientific, Pennsylvania) dyed red with oil red EGN (Aldrich Chemical Co., Wisconsin) into the center injection port in the top plate of the monolayer device. A minimum of 20 pore volumes of degassed Millipore water were allowed to pass through the monolayer of glass beads so that the injected PCE could equilibrate to the flow conditions. The pore volume of the monolayer of glass beads was 4.77 mL. To assess the effect of acoustic waves on PCE ganglia dissolution, a range of

acoustic frequencies and background volumetric fluid flow rates were applied at intervals of 20 pore volumes following a 20 pore volume period of flow without acoustic pressure. The various ganglia dissolutions experiments were conducted by progressively increasing the flow rate from low to high.

For each PCE ganglia dissolution experiment, effluent samples were collected at regular time intervals. The samples were immediately introduced into 2 mL vials (Kimble Glass, New Jersey) containing a known volume of *n*-pentane (Fisher Scientific, Pennsylvania). The dissolved aqueous phase PCE concentrations of the liquid samples were determined using a Hewlett Packard 5890 Series II gas chromatograph with an electron capture detector. The practical range of detection for PCE was from 0.5 to 80 mg/L. All of the samples collected contained PCE concentrations well within the specified detection range. The equilibrium aqueous solubility of PCE is 150 mg/L (Mackay *et al.*, 1992).

3.3. EXPERIMENTAL PROCEDURES FOR GANGLIA MOBILIZATION

The effect of acoustic waves on the mobilization of PCE ganglia was investigated with the same experimental apparatus used for the ganglia dissolution experiments and a digital camera (Olympus C2500L, Melville, New York) equipped with a combination of +1, +2, and +4, 49 mm macro lenses (Promaster Spectrum, Japan) positioned over the monolayer of glass beads. The digital camera was employed to record the actual paths of ganglia migration.

For each ganglia mobilization experiment, approximately 0.05 mL of PCE dyed red with oil red EGN was injected into the the center port of the monolayer device to form a single ganglion. The initial configuration of the PCE ganglion was recorded and the flow rate was incrementally increased until mobilization of the ganglion was achieved in the absence of acoustic waves. Subsequently, the fluid flow rate was discontinued and the new location/configuration of the ganglion was recorded. Acoustic waves with frequency $\phi = 125$ Hz were then applied to the monolayer of glass beads and the flow rate was incrementally increased until mobilization of the ganglion (or ganglia if dynamic breakup occurred) was again achieved. This procedure was repeated for a range of acoustic source pressures, p_s, and flow rates until all ganglia exited the monolayer.

The fluid flow conditions responsible for mobilizing PCE ganglia in the presence and absence of acoustic waves were compared with the dimensionless Capillary number, N_{Ca}, defined in (11). For the evaluation of N_{Ca} the average interstitial pore water velocity (U_w) was determined by dividing the volumetric flow rate (Q) by the cross sectional area (1.35 cm^2) and the porosity ($\theta = 0.39$) of the monolayer of glass beads. The dynamic fluid viscosity was set to $\mu_w = 1.0019$ cp. Furthermore, it was assumed that the

system examined in this study (glass-PCE-water) is a strongly water-wet system or equivalently that $\cos\beta = 1$ (Blunt *et al.*, 2002), and that the PCE-water interfacial tension is $\sigma_{ow} = 44.4$ dynes/cm (Mercer and Cohen, 1990).

4. Results and Discussion

4.1. ENHANCED GANGLIA DISSOLUTION RESULTS

The effluent concentrations collected in the absence and presence of acoustic waves for various flow rates are presented in Figure 5a as open and closed circles, respectively. Each experimental datum shown in Figure 5a corresponds to a different PCE dissolution experiment and represents the average concentration of three consecutive samples collected from the effluent stream at approximately the same time. The error bars indicate the experimental error evaluated as the standard deviation of the averaged concentrations. The experimental data are also presented in Figure 5b as the change in the average effluent concentration, which is defined as

$$\Delta\overline{C} = \frac{\overline{C}_a - \overline{C}_b}{\overline{C}_b}, \tag{12}$$

where $\overline{C}_a$ is the average effluent concentration collected in the presence of acoustic waves, and $\overline{C}_b$ is the average effluent concentration collected in the absence of acoustic waves. It should be noted that repeated ganglia dissolution experiments performed at several flow rates suggested that the experimental data were reproducible.

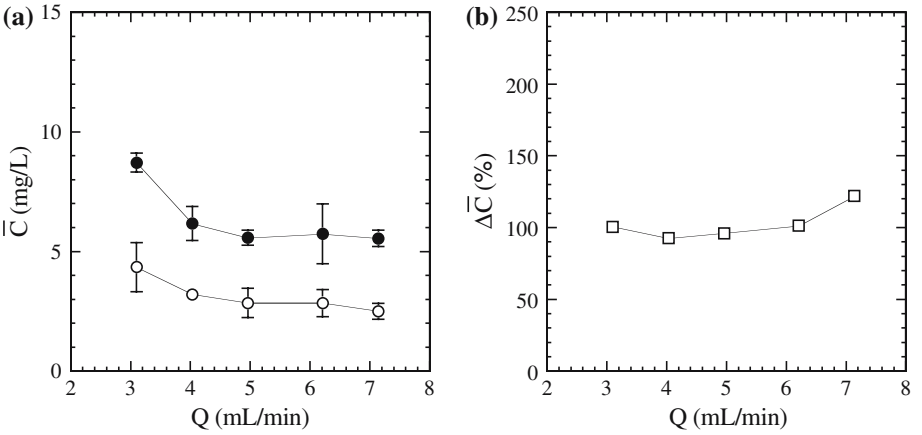

Figure 5. The effect of volumetric flow rate on the (a) average effluent concentrations in the absence (open circles) and presence (solid circles) of acoustic waves, and (b) change in average effluent concentrations. Here $\phi = 125$ Hz and $p_s = 3.68$ kPa.

The experimental results presented in Figure 5a indicate that all effluent concentrations measured in the absence and presence of acoustic waves are observed to slightly decrease with increasing flow rate. The most pronounced effluent concentration decrease occurs between the flow rates of approximately 3–4 mL/min, which are the lowest flow rates employed in this experimental study. Although the effluent concentrations are decreasing with increasing flow rates, the average mass transfer coefficient and consequently, the mass flux out of the monolayer is increasing with increasing flow rate (Bird *et al.*, 1960; Chrysikopoulos *et al.*, 2003). The effluent concentrations collected in the presence of acoustic waves are consistently greater than the effluent concentrations collected in the absence of acoustic waves. Figure 5b shows that $\Delta\overline{C}$ due to the addition of acoustic waves is consistently about 100%. However, the effect of increasing the background volumetric flow rate on $\Delta\overline{C}$ is essentially negligible for the flow rates used in this study. Clearly, the experimental data indicate that there is a significant enhancement in the dissolution of PCE ganglia in the presence of acoustic waves. The observed ganglia dissolution enhancement shown in Figure 5a and 5b is attributed to the oscillatory interstitial fluid velocity caused by the addition of acoustic waves. This oscillatory fluid velocity at the pore scale is probably changing the concentration gradient at the PCE ganglia–water interfaces, the effective molecular diffusion coefficient of dissolved PCE, the mass transfer coefficient, or a combination of all three processes. These results are in agreement with those reported for trichloroethylene (TCE) dissolution in one-dimensional packed columns (Vogler and Chrysikopoulos, 2004). However, $\Delta\overline{C}$ may be different for a NAPL with C_s substantially different than that of PCE. It is reported in the literature that for a multicomponent NAPL the greatest dissolution enhancement in the presence of acoustic waves is associated with the component of the NAPL mixture having the smallest C_s (Chrysikopoulos and Vogler, 1994).

The effect of acoustic wave frequency, ϕ, in the range of 75–225 Hz, on the effluent dissolved PCE concentration and $\Delta\overline{C}$ for a constant source pressure amplitude $p_s = 3.68$ kPa using a constant background volumetric fluid flow of $Q = 4.96$ mL/min, is shown in Figure 6. The average effluent dissolved PCE concentration in the absence of acoustic waves (open circles) and in the presence of acoustic waves (solid circles) as a function of ϕ is presented in Figure 6a. It should be noted that each pair of effluent dissolved concentration data (in the absence and presence of acoustic waves) presented in Figure 6a were obtained from a different experiment. Obviously, the effluent concentrations in the absence of acoustic waves are independent of ϕ and the observed variation is caused by slight differences in ganglia interfacial areas and geometries between different experiments. The greatest average effluent concentration in the presence of acoustic waves occurs at the lowest frequency used, $\phi = 75$ Hz. For frequencies

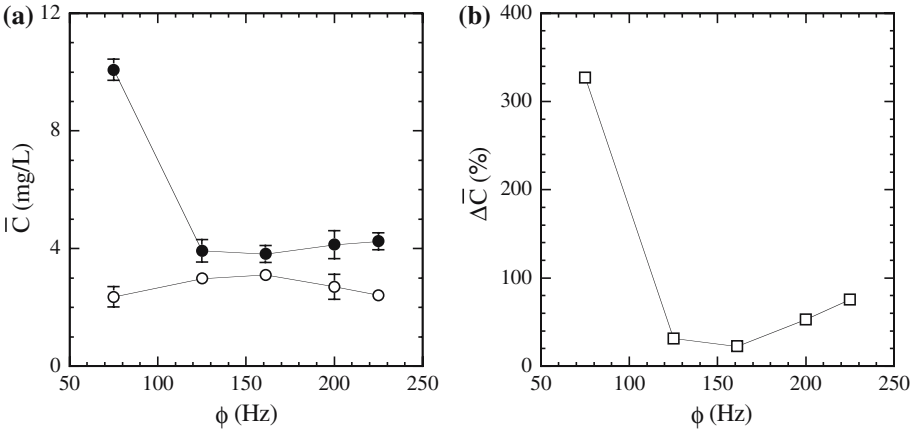

Figure 6. The effect of acoustic frequency on the (a) average effluent concentrations in the absence (open circles) and presence (solid circles) of acoustic waves, and (b) change in average effluent concentrations. Here $p_s = 3.68$ kPa and $Q = 4.96$ mL/min.

ranging from 125 to 225 Hz, the average effluent dissolved PCE concentrations exhibit a minor increase with increasing ϕ. Figure 6b shows that there is over a 300% increase in average effluent PCE concentrations for $\phi = 75$ Hz. The smallest $\Delta\overline{C}$ (23%) is observed at $\phi = 161$ Hz, and for higher frequencies $\Delta\overline{C}$ is observed to progressively increase to approximately 76% at $\phi = 225$ Hz. It should be noted that the relationship between $\Delta\overline{C}$ and ϕ shown in Figure 6b is similar to that observed during dissolution of multi-component ganglia (a three-component mixture containing PCE) in water saturated packed columns (Chrysikopoulos and Vogler, 2004).

The maximum $\Delta\overline{C}$ observed at the lowest frequency used for this work ($\phi = 75$ Hz) maybe attributed to the presence of the "slow wave," where the fluid within the pore space oscillates 180° out of phase with the porous media bulk matrix (Biot, 1956a,b). It has also been shown that lower frequency acoustic waves are less attenuated in porous media due to lower frictional forces along the pore walls (Biot, 1956a,b). The effluent pressure, recorded for the experiment with $\phi = 75$ Hz and a constant acoustic source pressure amplitude of $p_s = 3.68$ kPa, was 2.95 kPa. This effluent pressure p_e, is approximately three times greater than the p_e recorded for all other experiments with different frequencies. The effluent pressure recordings are an indication of the acoustic wave attenuation. Oscillatory pore water velocity is increasing with decreasing frequencies (Biot, 1956a,b), and it is responsible for the greatest observed $\Delta\overline{C}$ (see Figure 6b).

4.2. ENHANCED GANGLIA MOBILIZATION RESULTS

Figure 7 shows the evolution of a 12 pore PCE ganglion in the absence and presence of acoustic pressure waves. Note that the induced fluid flow

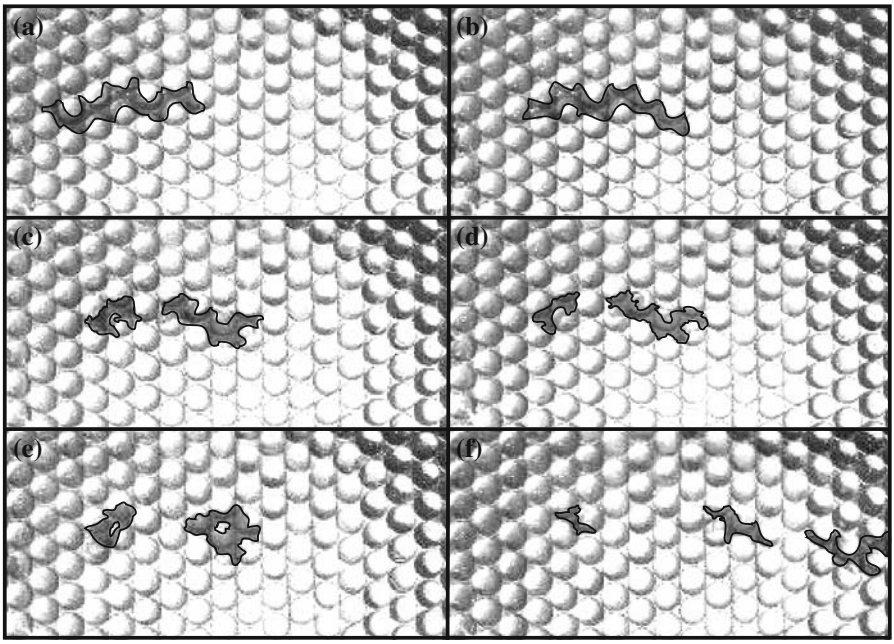

Figure 7. Evolution of a 12 pore PCE ganglion during its mobilization in the presence and absence of acoustic waves: (a) initial configuration of the ganglion at $p_s = 0.0\,\text{kPa}$, and $N_{Ca} = 0.0$, (b) mobilization in the absence of acoustic waves at $p_s = 0.0\,\text{kPa}$ and $N_{Ca} = 0.94 \times 10^{-2}$, (c) dynamic breakup in the presence of acoustic waves at $p_s = 7.35\,\text{kPa}$ and $N_{Ca} = 0.70 \times 10^{-2}$, (d) stagnation of the ganglia after elimination of of the acoustic waves at $p_s = 0.0\,\text{kPa}$ and $N_{Ca} = 1.16 \times 10^{-2}$, (e) shrinkage of the ganglia when acoustic waves were reintroduced at $p_s = 11.03\,\text{kPa}$ and $N_{Ca} = 0.73 \times 10^{-2}$, and (f) subsequent ganglia dynamic breakup and mobilization at the same values of $p_s = 11.03\,\text{kPa}$ and $N_{Ca} = 0.73 \times 10^{-2}$.

was in the direction from left to right. The initial ganglion configuration is shown in Figure 7a. After the ganglion was emplaced, the interstitial flow was initiated and progressively the flow rate, Q, was increased until mobilization was achieved at $N_{Ca} = 0.94 \times 10^{-2}$ in the absence of acoustic pressure waves (see Figure 7b). Subsequently, acoustic waves were applied with a pressure amplitude of $p_s = 7.35\,\text{kPa}$. The volumetric flow rate was incrementally increased until mobilization was attained. Figure 7c shows the ganglion to begin to split into two separate ganglia at $p_s = 7.35\,\text{kPa}$ and $N_{Ca} = 0.70 \times 10^{-2}$, which is lower than the N_{Ca} required for mobilization in Figure 7b. Following this dynamic breakup, the acoustic pressure waves were discontinued and Q was increased. Mobilization did not occur for the highest flowrate employed in this experimental study in the absence of acoustic pressure waves, which corresponds to $N_{Ca} = 1.16 \times 10^{-2}$ (see Figure 7d). Subsequently, acoustic pressure waves were again introduced with

$p_s = 11.03\,\text{kPa}$ and $N_{Ca} = 0.73 \times 10^{-2}$. Initially, no significant mobilization occurred. However, the larger of the two ganglia was observed to alter its shape and to shrink in the longitudinal direction (see Figure 7e). Eventually, the larger of the two ganglia was split again into two ganglia, which were mobilized (see Figure 7f). Note that in Figure 7e and 7f the values of p_s and N_{Ca} are identical.

Several additional mobilization experiments were conducted with various initial sizes of PCE ganglia. However, the results were similar to those presented in Figure 7 and suggest that that acoustic waves enhance ganglia mobilization. In the presence of acoustic waves, ganglia were mobilized at lower values of N_{Ca} or equivalently lower flow rates than in the absence of acoustic waves. Furthermore, dynamic breakup occurred more frequently in the presence of acoustics waves.

5. Summary

The effect of acoustic pressure waves on PCE ganglia dissolution and mobilization in a monolayer of glass beads was investigated. The effluent dissolved aqueous PCE concentration was observed to increase in the presence of acoustic waves compared to the case where acoustic waves were not applied. No significant ganglia dissolution enhancement was observed with increasing Q in the presence of acoustic waves. The greatest ganglia dissolution enhancement occurred at $\phi = 75\,\text{Hz}$, the lowest acoustic wave frequency used in this study. The enhanced dissolution may be attributed to an oscillatory pore water velocity component caused by the presence of acoustic waves.

Mobilization experiments indicated that in the presence of acoustic pressure waves PCE ganglia were mobilized at lower N_{Ca} or equivalently at lower flow rates than the case were acoustic waves were not applied to the monolayer device. Furthermore, it was observed that more dynamic breakup or splitting of the PCE ganglia occurred in the presence of acoustic waves.

The results of this research suggest that acoustic waves may be used to enhance ganglia dissolution, to improve ganglia mobilization as well as to increase ganglia dynamic breakup. Ganglia splitting into smaller discontinuous blobs is beneficial in aquifer remediation applications because dissolution rates increase with greater DNAPL-water interfacial areas.

Acknowledgements

This work was funded by the USA National Science Foundation under NSF Award Number BES-0329398. The content of this manuscript does not necessarily reflect the views of the agency and no official endorsement should be inferred.

References

Abriola, L. M., Dekker, T. J. and Pennell, K. D.: 1993, Surfactant-enhanced solubilization of residual dodecane in soil columns. 2. Mathematical modeling, *Environ. Sci. Technol.* **27**(12), 2341–2351.

Avraam, D. G. and Payatakes, A. C.: 1995, Flow regimes and relative permeabilities during steady-state two-phase flow in porous media, *J. Fluid Mech.* **293**, 207–236.

Avraam, D. G., Kolonis, G. B., Roumeliotis, T. C., Constantinides, G. N. and Payatakes, A. C.: 1994, Steady-state two-phase flow through planar and nonplanar model porous media, *Transport Porous Media* **16**, 75–101.

Bear, J.: 1972, *Dynamics of Fluids in Porous Media*, Dover, New York.

Bird, R. B., Stewart, W. E. and Lightfoot, E. N.: 1960, *Transport Phenomena*, Wiley, New York.

Blunt, M., King, M. J.: 1992, Simulation and theory of two-phase flow in porous media, *Phys. Rev. A* **46**(12), 7680–7699.

Blunt, M. J., Jackson, M. D., Piri, M. and Valvatne, P. H.: 2002, Detailed physics, predictive capabilities and macroscopic consequences for pore-network models of multiphase flow, *Adv. Water Res.* **25**, 1069–1089.

Boving, T. B., Waang, X. and Brusseau, M. L.: 1999, Cyclodextrin-enhanced solubilization and removal of residual-phase chlorinated solvents from porous media, *Environ. Sci. Technol.* **33**, 764–770.

Bradford, S. A., Rathfelder, K. M., Lang, J. and Abriola, L. M.: 2003, Entrapment and dissolution of DNAPLs in heterogeneous porous media, *J. Contam. Hydrol.* **67**, 133–157.

Brandes, D. and Farley, K. J.: 1993, Importance of phase behavior on the removal of residual DNAPLs from porous media by alcohol flooding, *Water Environ. Res.* **65**(7), 869–878.

Buckley, J. S.: 1991, Multiphase displacements in micromodels, in N. R. Morrow (ed.), *Interfacial Phenomena in Petroleum Recovery,* Surfactant Science Series, Vol. 36, Marcel Dekker, New York, pp. 157–189.

Chaudhry, G. R.: 1994, *Biological Degradation and Bioremediation of Toxic Chemicals*, Dioscorides Press, Portland.

Chomsurin, C. and Werth, C. J.: 2003, Analysis of pore-scale nonaqueous phase liquid dissolution in etched silicon pore networks, *Water Resour. Res.* **39**(9), 1265, doi:10.1029/2002WR001643.

Chrysikopoulos, C. V.: 1995, Three-dimensional analytical models of contaminant transport from nonaqueous phase liquid pool dissolution in saturated subsurface formations, *Water Resour. Res.* **31**(4), 1137–1145.

Chrysikopoulos, C. V. and Vogler, E. T.: 2004, Acoustically enhanced multicomponent NAPL ganglia dissolution in water saturated packed columns, *Environ. Sci. Technol.* **38**(10), 2940–2945.

Chrysikopoulos, C. V., Voudrias, E. A. and Fyrillas, M. M.: 1994, Modeling of contaminant transport resulting from dissolution of nonaqueous phase liquid pools in saturated porous media, *Transport Porous Media* **16**(2), 125–145.

Chrysikopoulos, C. V., Hsuan, P.-Y. and Fyrillas, M. M.: 2002, Bootstrap estimation of the mass transfer coefficient of a dissolving nonaqueous phase liquid pool in porous media, *Water Resour. Res.* **38**(3), 1026, doi:10.1029/2001WR000661.

Chrysikopoulos, C. V., Hsuan, P.-Y., Fyrillas, M. M. and Lee, K. Y.: 2003, Mass transfer coefficient and concentration boundary layer thickness for a dissolving NAPL pool in porous media, *J. Hazard. Mater.* **B97**, 245–255.

Cohen, R. M. and Mercer, J. W.: 1993, *DNAPL Site Evaluation*, CRC Press, Florida.

Conrad, S. H., Wilson, J. L., Mason, W. R. and Peplinski, W. J.: 1992, Visualization of residual organic liquid trapped in aquifers, *Water Resour. Res.* **28**(2), 467–478.

Cussler, E. L.: 1984, *Diffusion – Mass Transfer in Fluid Systems*, Cambridge University Press, Cambridge.

Dawson, H. E.: 1992, Entrapment and mobilization of residual halogenated organic liquids in saturated aquifer material, Ph.D. Dissertation, Stanford University.

Dawson, H. E., and Roberts, P. V.: 1997, Influence of viscous, gravitational, and capillary forces on DNAPL saturation, *Ground Water* **35**(2), 261–269.

de la Cruz, V. and Spanos, T. J. T.: 1983. Mobilization of oil ganglia, *AIChE J.* **29**(5), 854–858.

Dela Barre, B. K., Harmon, T. C. and Chrysikopoulos, C. V.: 2002, Measuring and modeling the dissolution of nonideally shaped dense nonaqueous phase Liquid (NAPL) pools in saturated porous media, *Water Resour. Res.* **38**(8), 1133, doi:10.1029/2001 WR000444.

Dias, M. M. and Payatakes, A. C.: 1986, Network models for two-phase flow in porous media, Part 2. Motion of oil ganglia, *J. Fluid Mech.* **164**, 337–358.

Dillard, L. A. and Blunt, M. J.: 2000, Development of a pore network simulation model to study nonaqueous phase liquid dissolution, *Water Resour. Res.* **36**(2), 439–454.

Dullien, F. A. L.: 1979, *Porous Media. Fluid Transport and Pore Structure*, Academic Press, New York.

Fenwick, D. H. and Blunt, M. J.: 1998, Three-dimensional modeling of three phase imbibition and drainage, *Adv. Water Res.* **21**(2), 121–143.

Fortin, J., Jury, W. A. and Anderson, M. A.: 1997, Enhanced removal of trapped nonaqueous phase liquids from saturated soil using surfactant solutions, *J. Contam. Hydrol.* **24**(3–4), 247–267.

Grubb, D. G. and Sitar, N.: 1999, Mobilization of trichloroethene (TCE) during ethanol flooding in uniform and layered sand packs under confined conditions, *Water Resour. Res.* **35**(11), 3275–3289.

Held, R. J. and Celia, M. A.: 2001, Pore-scale modeling and upscaling of nonaqueous phase liquid mass transfer, *Water Resour. Res.* **37**(3), 539–549.

Hinkley, E. R., Dias, M. M. and Payatakes, A. C.: 1987, On the motion of oil ganglia in porous media, *PhysicoChem. Hydrodyn.* **8**(2), 185–211.

Hofstee, C., Ziegler, C. G., Trötschler, O. and Braun, J.: 2003, Removal of DNAPL contamination from the saturated zone by the combined effect of vertical upward flushing and density reduction, *J. Contam. Hydrol.* **67**, 61–78.

Imhoff, P. T., Gieyzer, S. N., McBride, J. F., Vancho, L. A., Okuda, I. and Miller, C. T.: 1995, Cosolvent-enhanced remediation of residual dense nonaqueous phase liquids; Experimental investigation, *Environ. Sci. Technol.* **29**(8), 1966–1976.

Jia, C., Shing, K. and Yortsos, Y. C.: 1999, Visualization and simulation of non-aqueous phase liquids solubilization in pore networks, *J. Contam. Hydrol.* **35**, 363–387.

Keller, A. A., Blunt, M. J. and Roberts, P. V.: 1997, Micromodel observation of the role of oil layers in three-phase flow, *Transport Porous Media* **26**, 277–297.

Kennedy, C. A. and Lennox, W. C.: 1997, A pore-scale investigation of mass transport from dissolving DNAPL droplets, *J. Contam. Hydrol.* **24**, 221–246.

Khachikian, C. and Harmon, T. C.: 2000, Nonaqueous phase liquid dissolution in porous media: Current state of knowledge and research needs, *Transport Porous Media* **38**, 3–28.

Kim, T.-J. and Chrysikopoulos, C. V.: 1999, Mass transfer correlations for nonaqueous phase liquid pool dissolution in saturated porous media, *Water Resour. Res.* **35**(2), 449–459.

Knutson, C. E., Werth, C. J. and Valocchi, A. J.: 2001, Pore-scale modeling of dissolution from variably distributed nonaqueous phase liquid blobs, *Water Resour. Res.* **37**(12), 2951–2963.

Lenormand, R.: 1990, Liquids in porous media, *J. Phys.: Condens. Matter* **2**, SA79–SA88.

Lenormand, R. and Zarcone, C.: 1988, Physics of blob displacement in a two-dimensional porous medium, *SPE Form. Eval.* (3), 271–275.

Lenormand, R., Zarcone, C. and Sarr, A.: 1983, Mechanism of displacement of one fluid by another in a network of capillary ducts, *J. Fluid Mech.* **135**, 337–353.

Li, X. and Yortsos, Y. C.: 1995, Visualization and simulation of bubble growth in pore networks, *AIChE J.* **41**, 214–223.

Mackay, D., Shiu, W. Y., Ma, K. C.: 1992, *Illustrated Handbook of Physical-chemical Properties and Environmental Fate for Organic Chemicals, Volume 3, Volatile Organic Chemicals*, Lewis Publishers, Chelsea, Michigan.

Mason, A. R. and Kueper, B. H.: 1996, Numerical simulation of surfactant-enhanced solubilization of pooled DNAPL, *Environ. Sci. Technol.* **30**(11), 3205–3215.

Mayer, A. S. and Miller, C. T.: 1993, An experimental investigation of pore-scale distributions of nonaqueous phase liquids at residual saturation, *Transport Porous Media* **10**, 57–80.

Mercer, J. W. and Cohen, R. M.: 1990, A review of immiscible fluids in the subsurface: Properties, models, characterization and remediation, *J. Contam. Hydrol.* **6**(2), 107–163.

Morrow, N. R., Chatzis, I. and Taber, J. J.: 1988, Entrapment and mobilization of residual oil in bead packs, *SPE Form. Eval.* (8), 927–934.

Ng, K. M., Davis, H. T. and Scriven, L. E.: 1978, Visualization of blob mechanics in flow through porous media, *Chem. Eng. Sci.* **33**, 1009–1017.

Payatakes, A. C.: 1982, Dynamics of oil ganglia during immiscible displacement in waterwet porous media, *Ann. Rev. Fluid Mech.* **14**, 365–393.

Pennell, K. D., Pope, G. A. and Abriola, L. M.: 1996, Influence of viscous and buoyancy forces on the mobilization of residual tetrachloroethylene during surfactant flushing, *Environ. Sci. Technol.* **30**, 1328–1335.

Pennell, K. D., Jin, M., Abriola, L. M. and Pope, G. A.: 1994, Surfactant enhanced remediation of soil columns contaminated by residual tetrachloroethylene, *J. Contam. Hydrol.* **16**, 35–53, 1994.

Powers, S. E., Loureiro, C. O., Abriola, L. M. and Weber, W. J., Jr.: 1991, Theoretical study of the significance of non-equilibrium dissolution on nonaqueous phase liquids in subsurface systems, *Water Resour. Res.* **27**, 463–477.

Rao, P. S. C., Annable, M. D., Sillan, R. K., Dai, D. P., Hatfield, K., Graham, W. D., Wood, A. L. and Enfield, C. G.: 1997, Field-scale evaluation of in-situ cosolvent flushing for remediation of a shallow unconfined aquifer contaminated with residual LNAPL, *Water Resour. Res.* **33**(12), 2673–2686.

Reddi, L. N. and Challa, S.: 1994, Vibratory mobilization of immiscible liquid ganglia in sands, *J. Environ. Eng.* **120**(5), 1170–1190.

Reddi, L. N., Menon, S. and Plant, A.: 1998, Pore-scale investigations on vibratory mobilization of LNAPL ganglia, *J. Hazard. Mater.* **62**, 211–230.

Reddi, L. N. and Wu, H.: 1996, Mechanisms involved in vibratory destabilization of NAPL ganglia in sands, *J. Environ. Eng.* **122**(12), 1115–1119.

Roberts PM, Sharma A, Uddameri V, Monagle M, Dale DE, Steck LK.: 2001, Enhanced DNAPL transport in a sand core during dynamic stress simulation, *Environ. Eng. Sci.* **18**(2), 67–79.

Saba, T., Illangasekare, T. H. and Ewing, J.: 2001, Investigation of surfactant-enhanced dissolution of entrapped nonaqueous phase liquid chemicals in a two-dimensional groundwater flow field, *J. Contam. Hydrol.* **51**, 63–82.

Sahloul, N. A., Ioannidis, M. A. and Chatzis, I.: 2002, Dissolution of residual non-aqueous phase liquids in porous media: pore-scale mechanisms and mass transfer rates, *Adv. Water Res.* **25**, 33–49.

Scheidegger, A. E.: 1960, *The Physics of Flow Through Porous Media*, Macmillan Co., New York.

Seagren, E. A., Rittmann, B. E. and Valocchi, A. J.: 1994, Quantitative evaluation of the enhancement of NAPL-pool dissolution by flushing and biodegradation, *Environ. Sci. Technol.* **28**(5), 833–839.

Tatalovich, M. E., Lee, K. Y. and Chrysikopoulos, C. V.: 2000, Modeling the transport of contaminants originating from the dissolution of DNAPL pools in aquifers in the presence of dissolved humic substances, *Transport Porous Media* **38**, 93–115.

Tsakiroglou, C. D., Theodoropoulou, M. A. and Karoutsos, V.: 2003, Nonequilibrium capillary pressure and relative permeability curves of porous media, *AIChE J.* **49**(10), 2472–2486.

Vogler, E. T. and Chrysikopoulos, C. V.: 2002, Experimental investigation of acoustically enhanced solute transport in porous media, *Geophys. Res. Lett.* **29**(15), 1710, doi:10.1029/2002 GL015304.

Vogler, E. T. and Chrysikopoulos, C. V.: 2004, An experimental study of acoustically enhanced NAPL dissolution in porous media, *AIChE J.* **50**(12), 3271–3280.

Wilson, J. L., Conrad, S. H., Mason, W. R. and Peplinski, W.: 1990, Laboratory investigation of residual liquid organics from spills, leaks, and the disposal of hazardous wastes in groundwater, *EPA/600/6-0/004*, U.S. Environmental Protection Agency, Narraganset, R. I.

Zhao, W. and Ioannidis, M. A.: 2003, Pore network simulation of the dissolution of a single-component wetting nonaqueous phase liquid, *Water Resour. Res.* **39**(10), 1291, doi:10.1029/2002WR001861.